RESEARCH ARTICLE

Figures and figure supplements

Cross-modal interaction of human alpha activity does not reflect inhibition of early sensory processing in a frequency-tagging study using EEG and MEG

Marion Brickwedde *et al.*

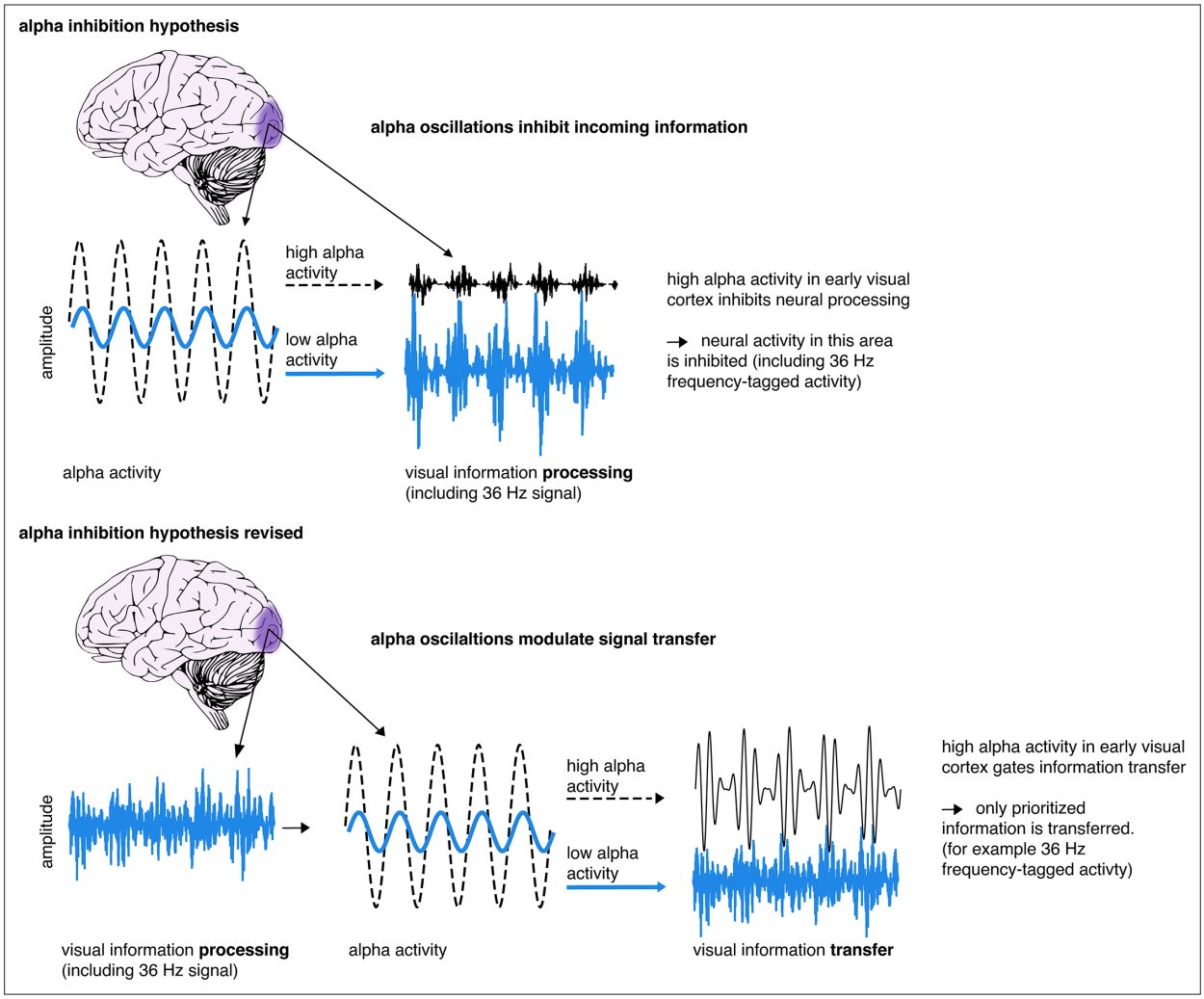

Figure 1. Illustration of the alpha inhibition hypothesis. The alpha inhibition hypothesis suggests that occipital alpha inhibits visual information processing in a phasic manner. If alpha activity is high, it suggests that neural processing in the cortical area is inhibited (***Foxe et al., 1998***; ***Jensen and Mazaheri, 2010***; ***Klimesch et al., 2007***). We propose a revision of this hypothesis, whereby alpha activity exerts its phasic inhibition to regulate information transfer, creating enhanced signal packages of prioritised information (see also ***Yang et al., 2023***; ***Zhigalov and Jensen, 2020***; ***Zumer et al., 2014***). This way, irrelevant or distracting information is inhibited through a block of transfer, rather than through blocking of incoming sensory information.

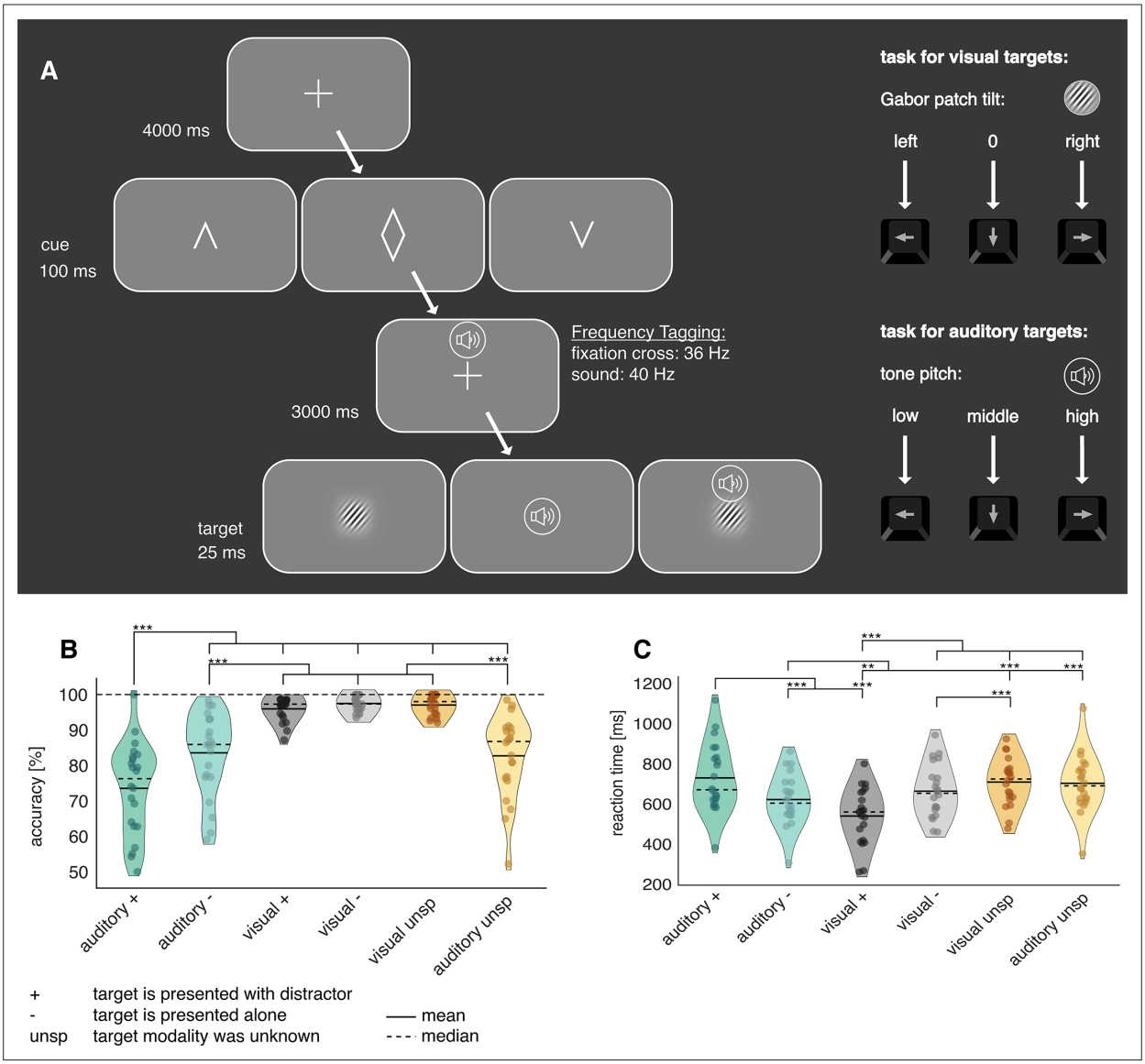

Figure 2. Illustration of the cross-model discrimination task in study 1. (**A**) Trials were separated by a 4 s interval, in which a fixation cross was displayed. A brief central presentation of the cue (100 ms) initiated the trial, signalling the target modality (see figure above from left to right: auditory, non-specific, visual). In the cue-to-target interval, the fixation cross was frequency-tagged at 36 Hz. At the same time, a sound was displayed over headphones, which was frequency-tagged at 40 Hz. Both tones and fixation cross contained no task-relevant information. The target, consisting either of a static Gabor patch or a tone, was presented for 25ms. Participants had to differentiate via button presses between three different Gabor rotations or tone pitches, respectively. In 50% of auditory and visually cued trials, a distractor in form of a random pitch or rotation of the un-cued modality was presented alongside the target. (**B, C**) Analysis of task accuracy and reaction time indicates increased difficulty of auditory targets. (**B**) Task accuracy compared between all six experimental conditions reveals a drop in accuracy for responses to auditory targets. (**C**) Reaction times of correct trials compared between all six experimental conditions. The slowest reaction times are observable following auditory targets alongside visual distractors. There was an attentional benefit of cues for reaction times and a distractor cost for accuracy and reaction times (see ***Figure 2—figure supplement 1***) N=22; *** sig <0.001; ** sig.<0.01; * sig.<0.05.

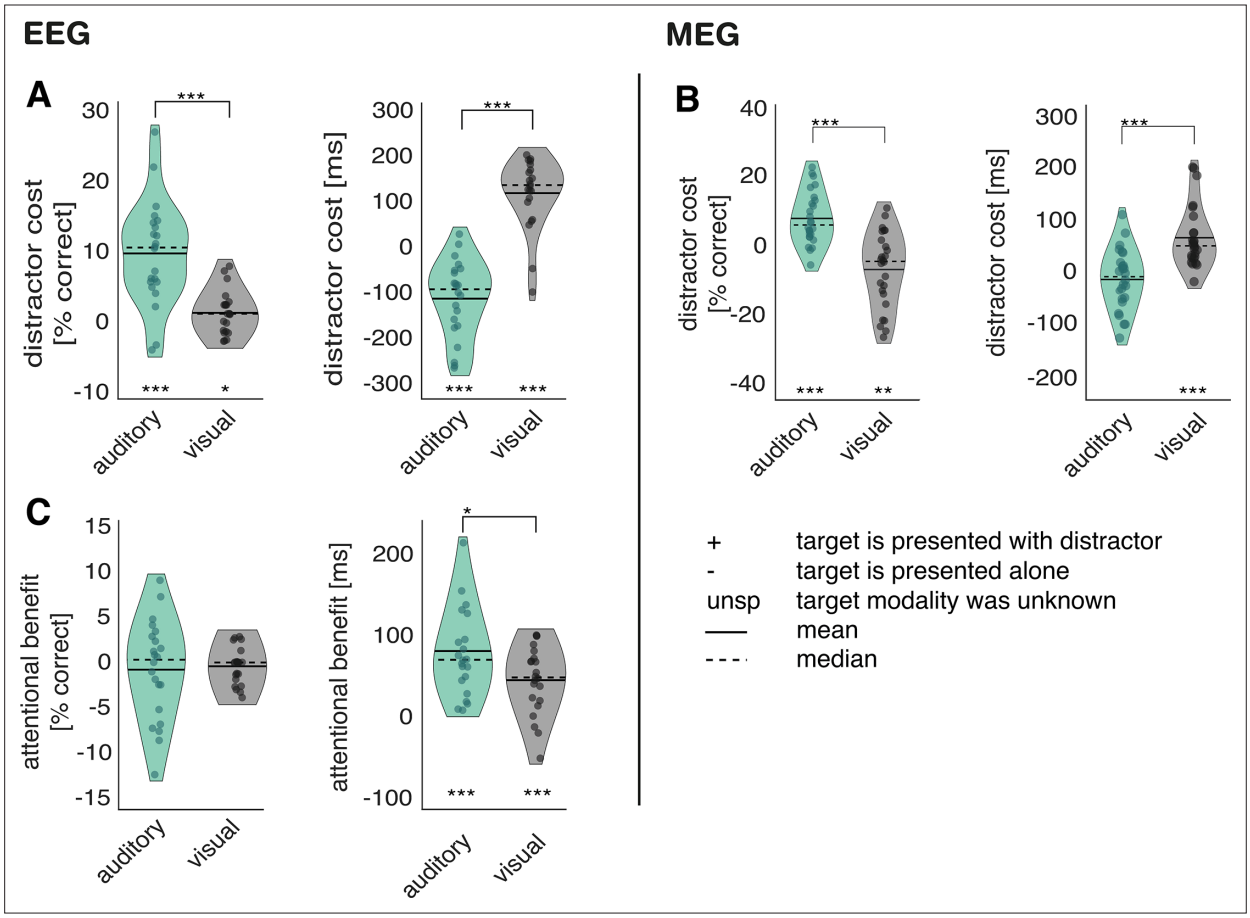

Figure 2—figure supplement 1. Distractor cost and attentional benefit.

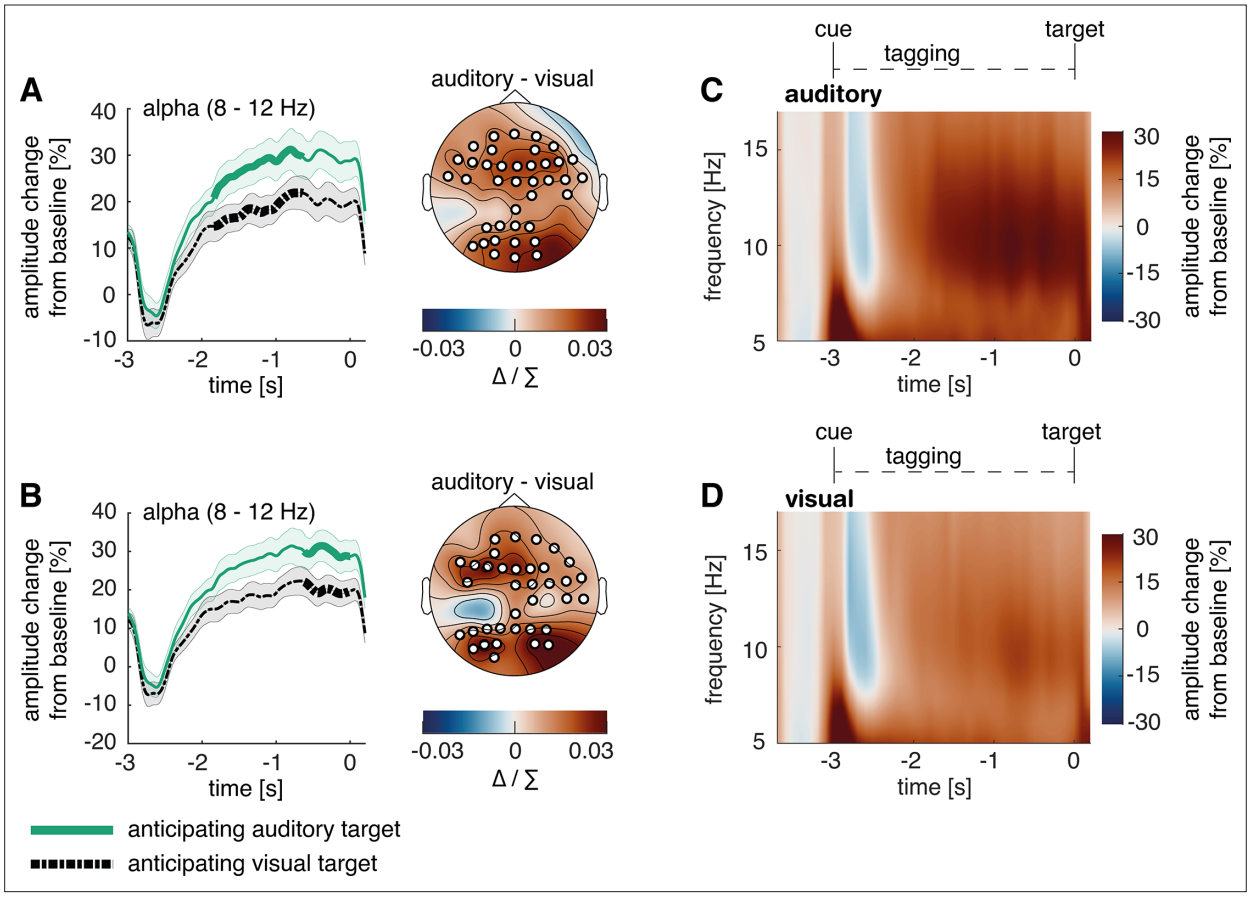

Figure 3. Post-cue modality-specific modulation of alpha power in anticipation of an auditory versus a visual target. (**A, B**) The time course of post-cue alpha power. Cluster permutation analysis resulted in two condition effects, both indicating heightened alpha activity when expecting an auditory compared to a visual target (**A**: p<0.01; **B**: p<0.01). For a comparison to trials with non-specific cues, see ***Figure 3—figure supplement 1***. (**C, D**) Time-frequency representation of power in the cue-to-target interval. A greater increase in alpha power was observed when expecting an auditory target (average over significant electrodes for the condition difference in **A**). *Note:* Cluster electrodes are marked in white. Shading represents standard error from the mean; Δ / ∑ represents (a-b)/(a+b) normalisation.

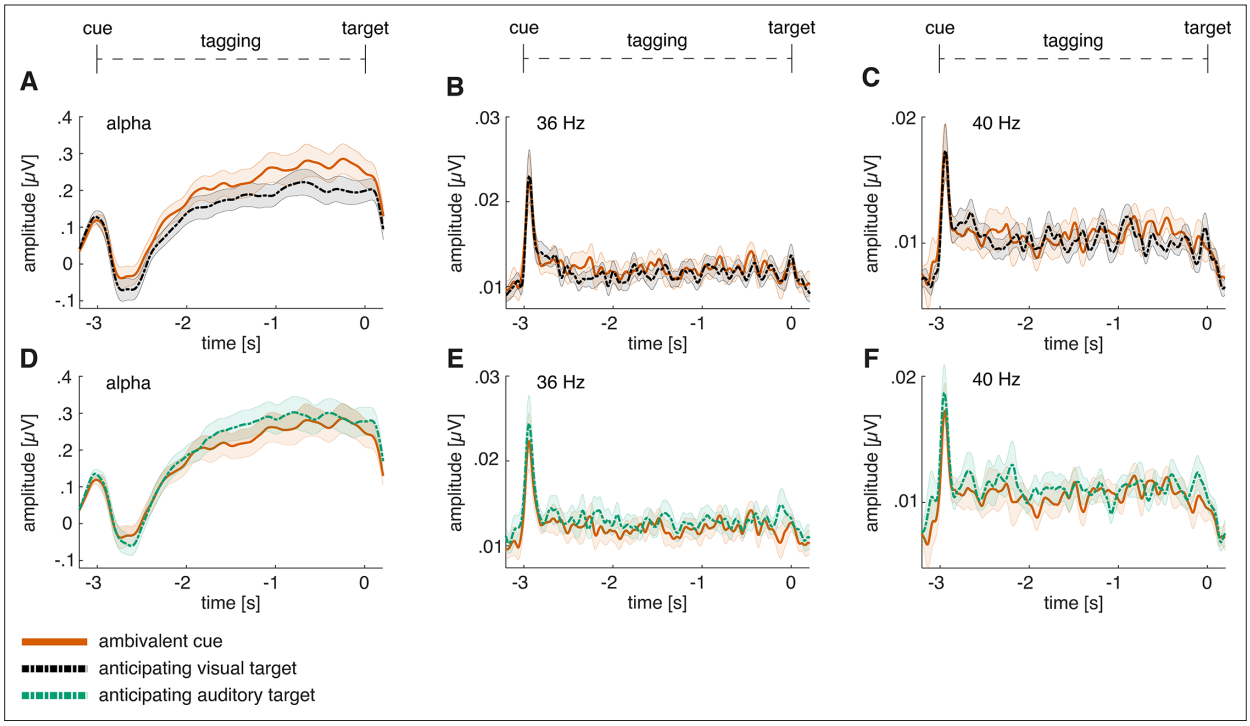

Figure 3—figure supplement 1. Time course of alpha activity and frequency-tagging responses for the non-specific compared to the visually-cued condition.

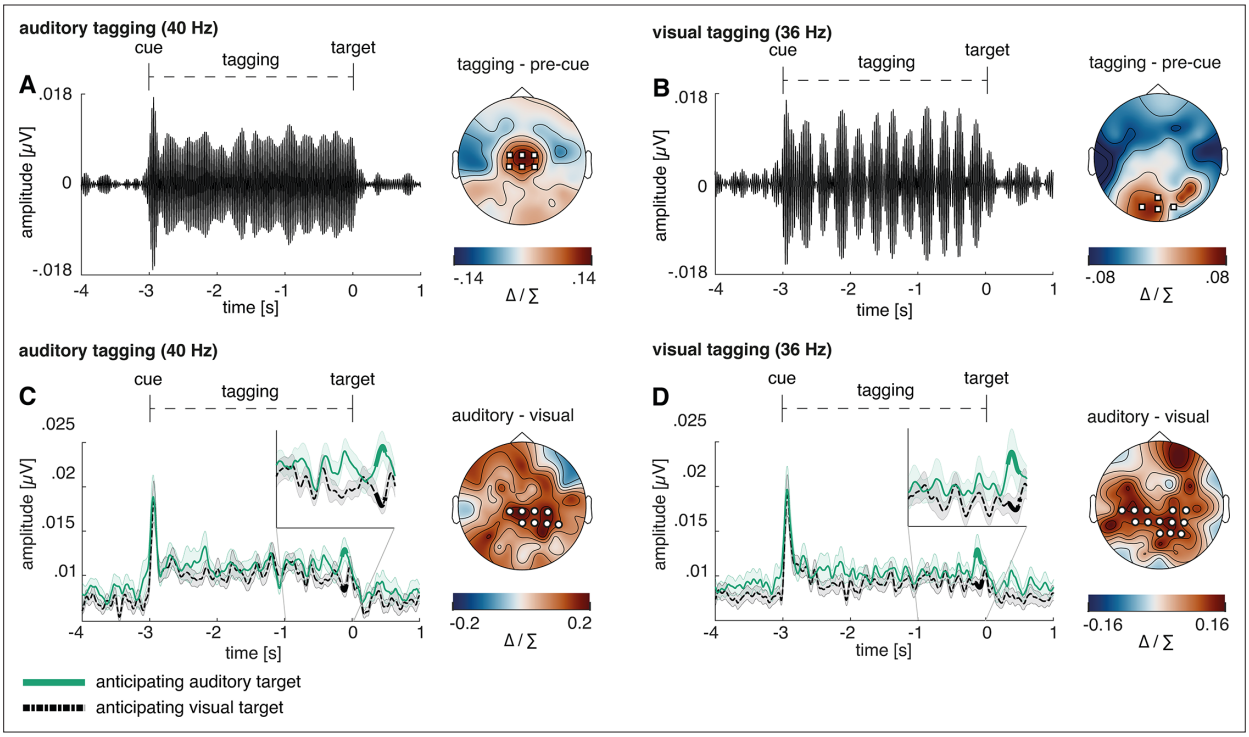

Figure 4. Increase in amplitude of both visual and auditory frequency-tagged responses when anticipating visual or auditory targets. Event-related potentials and scalp topographies reveal distinct modality-specific responses at the tagged frequencies. (**A**) Auditory steady-state evoked potential (ASSEP) averaged over six central electrodes displaying the highest 40 Hz power (Cz, FC1, FC2, C1, C2, FCz; marked with white squares). (**B**) Visual steady-state evoked potential (VSSEP) averaged over four occipital electrodes displaying the highest 36 Hz power (POz, O1, O2, Oz; marked with white squares). (**C**) The Hilbert envelope of the 40 Hz ASSEP reveals an increase shortly before target onset when anticipating an auditory compared to a visual target (p=0.041); (**D**) the Hilbert envelope of the 36 Hz VSSEP likewise reveals an increase shortly before target onset when anticipating an auditory compared to a visual target (p=0.014). For individual power spectra across conditions, see ***Figure 4—figure supplements 1 and 2***. For a comparison to trials with non-specific cues, see ***Figure 3—figure supplement 1***. *Note*: Cluster electrodes are marked in white. Shading represents standard error from the mean. Δ / ∑ represents (a-b)/(a+b) normalisation.

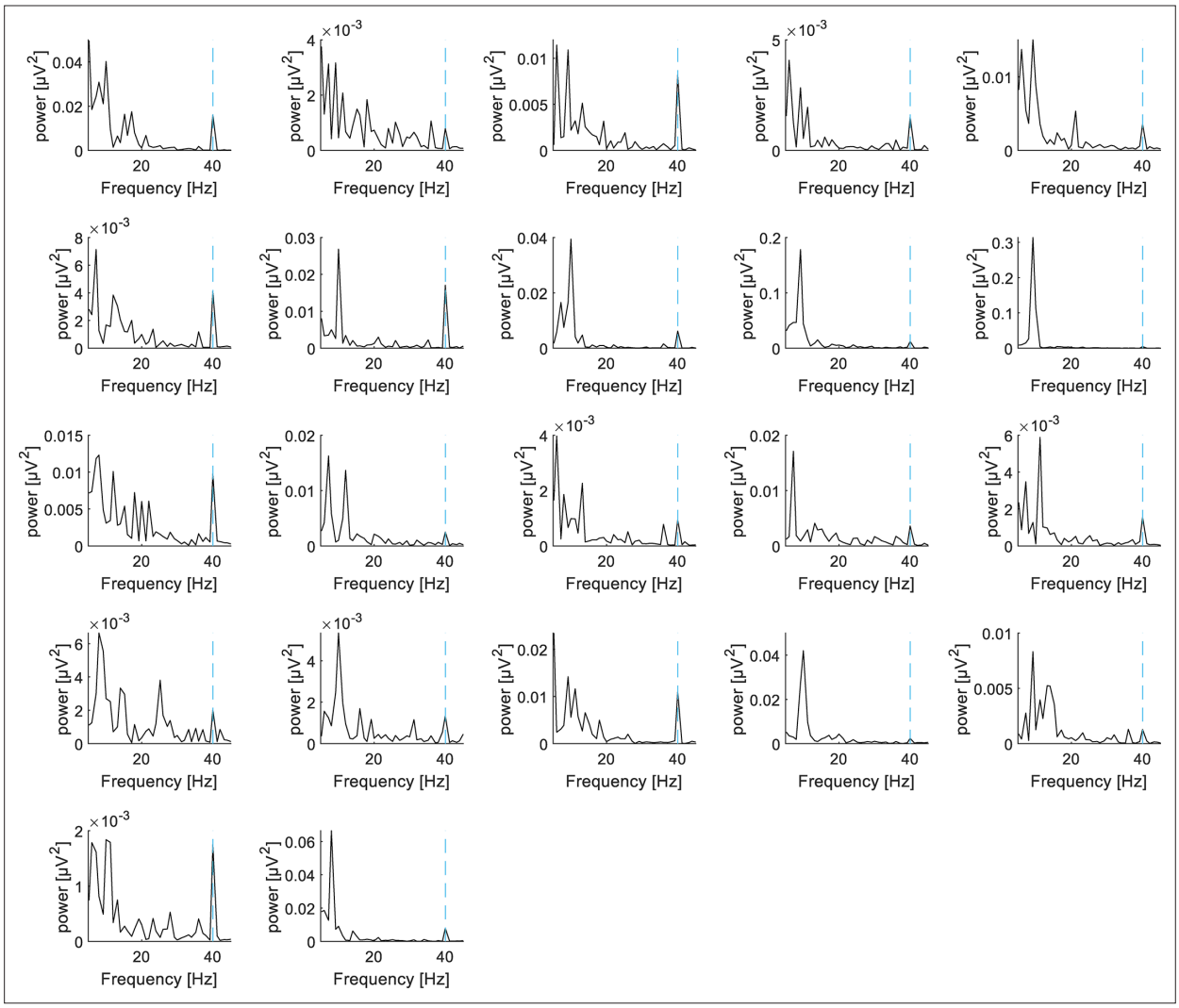

Figure 4—figure supplement 1. Individual ERP power spectra of the cue-to-target interval when anticipating an auditory target in the EEG-study.

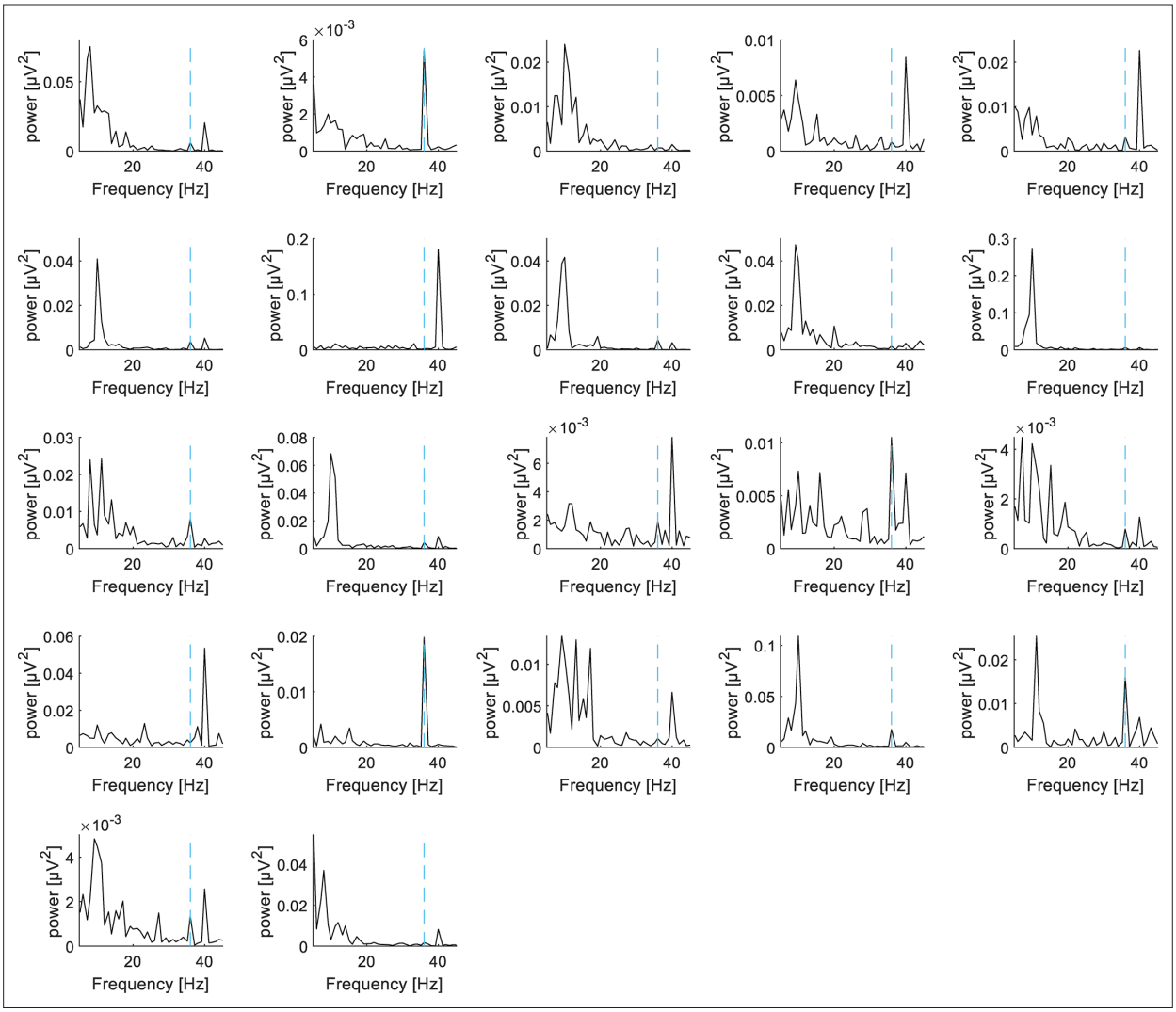

Figure 4—figure supplement 2. Individual ERP power spectra of the cue-to-target interval when anticipating a visual target in the EEG-study.

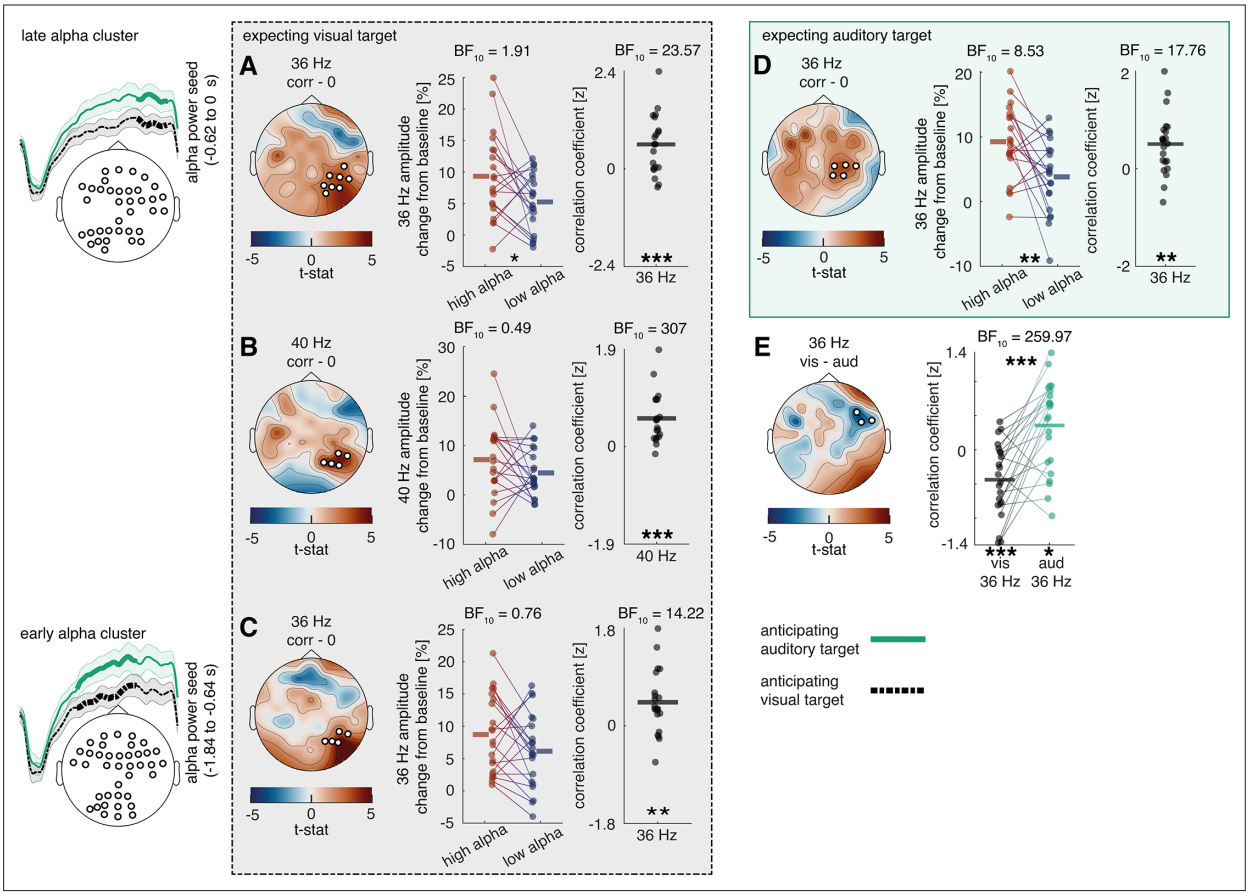

Figure 5. Relationship between cue-induced alpha modulation and amplitude of frequency-tagged responses in study 1. Previously obtained alpha clusters (see ***Figure 3***) were correlated over trials with auditory 40 Hz and visual 36 Hz clusters (see ***Figure 4***), where alpha electrodes/sensors were applied as seeds. The analysis was performed using a cluster-permutation approach, testing a correlation model against a 0-correlation model. Clusters significantly diverging from the 0-correlation model are presented topographically. Additionally, median splits between high and low alpha trials as well as correlation coefficients of these clusters are displayed for all participants. (**A, B**) A positive correlation is visible between alpha activity in the last 400 ms and steady state potentials shortly before target onset when expecting a visual target (visual 36 HZ: p=0.013; 40 Hz: p=0.009). (**D**) When expecting an auditory target, there is a positive correlation between alpha activity in the last 400 ms and visual 36 Hz activity shortly before target onset (p=0.010). (**E**) The correlation between alpha activity 400 ms and visual 36 Hz activity shortly before target onset changes its direction depending on whether an auditory or a visual target is expected (p=0.037). (**C**) A positive correlation is also visible between alpha activity as early as ~1200 ms to 400 ms and visual 36 Hz activity shortly before target onset when expecting a visual target (p=0.016). N=22; *** sig <0.001; ** sig <0.01; * sig <0.05.+sig.<0.1.

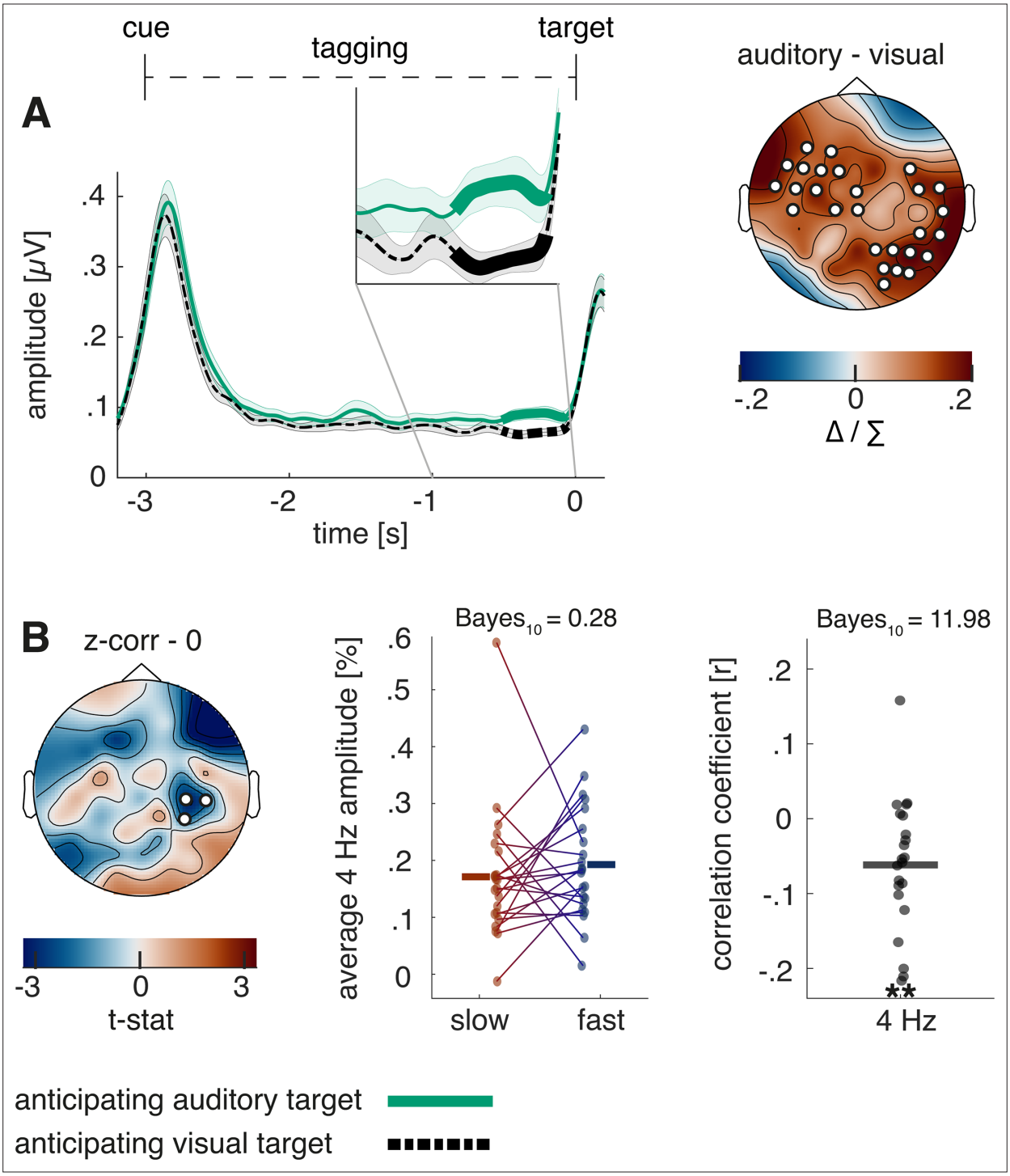

Figure 6. Steady-state response in the intermodulation frequency and its behavioural relevance. (**A**) The Hilbert envelope of the 4 Hz steady-state response reveals an increase shortly before target onset when anticipating an auditory compared to a visual target ($p<0.01$). (**B**) There is a trial-by-trial correlation between 4 Hz activity and reaction time when a visual target without distractor was presented. The correlation is further illustrated by a median split between fast and slow reaction time trials as well as by correlation coefficients for each participant. N=22; ** sig.<0.01.

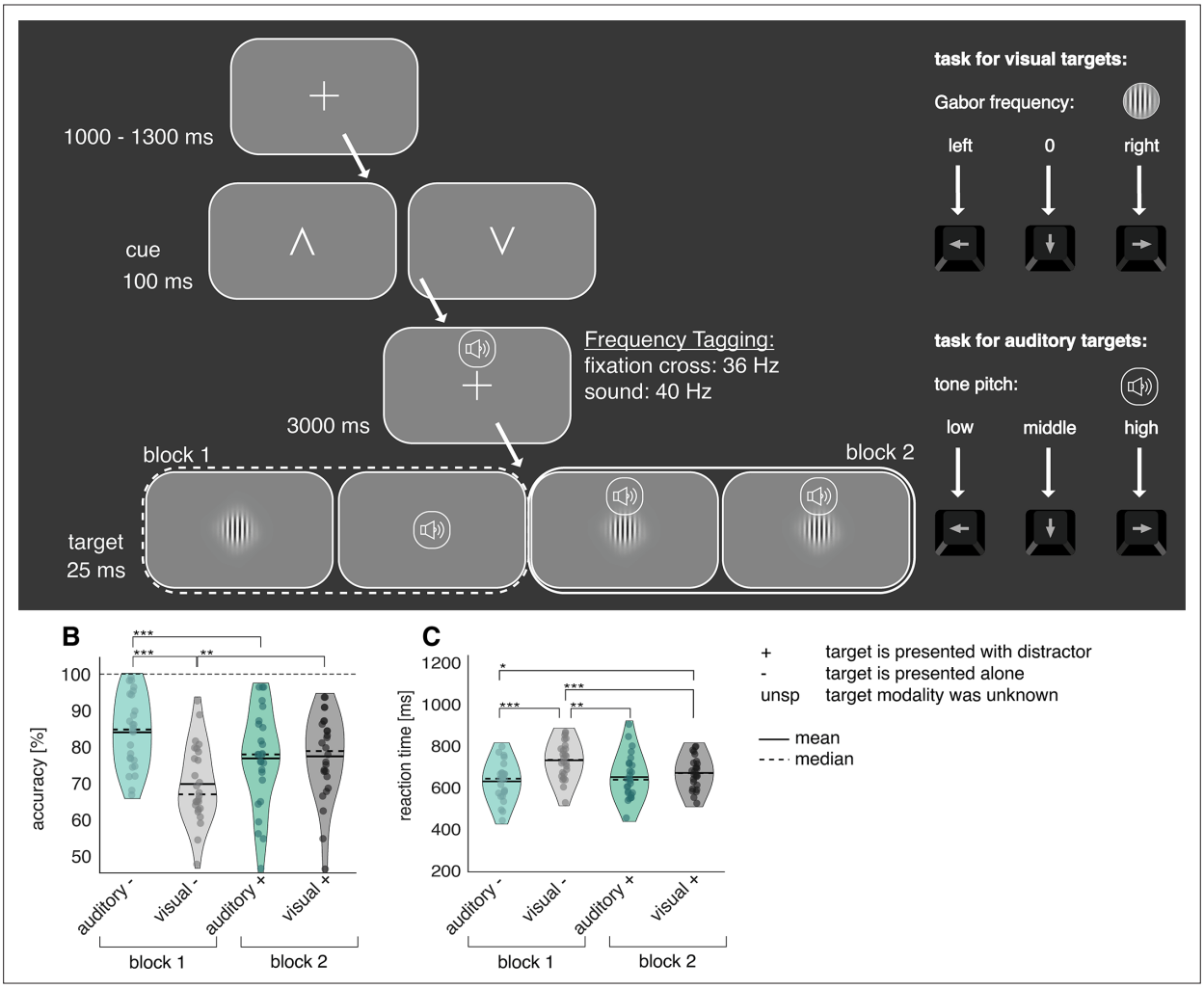

Figure 7. Illustration of the cross-model discrimination task in study 2. (**A**) Trials were separated by a 1–1.3 s interval, in which a fixation cross was displayed. A brief central presentation of the cue (100 ms) initiated the trial, signalising the target modality (from left to right: auditory, visual). In the cue-to-target interval, the fixation cross was frequency-tagged at 36 Hz. At the same time, a sound was displayed over headphones, which was frequency-tagged at 40 Hz. Both tones and fixation cross contained no task-relevant information. The target, consisting either of a static Gabor patch or a tone, was presented for 25 ms. Participants had to differentiate via button presses between three different Gabor stripe frequencies or tone pitches, respectively. In block 2, a distractor in the form of a random sound or Gabor patch of the un-cued modality was always presented alongside the target. Fixation was confirmed with an eye-tracker (see ***Figure 7—figure supplement 1***). (**B, C**) Analysis of task accuracy and reaction time indicates comparable difficulties in block 2. (**B**) Task accuracy differences were only observable in the first block without distractors. (**C**) Reaction times to visual targets in the first block were strongly increased compared to all other conditions. In the second block, no significant difference in reaction times was observable. A distractor cost was found for accuracy as well as reaction times when expecting a visual target. When expecting an auditory target, distractor cost manifested mainly in reduced accuracy (see ***Figure 2—figure supplement 1***). N=27; *** sig <0.001; ** sig.<0.01; * sig.<0.05.

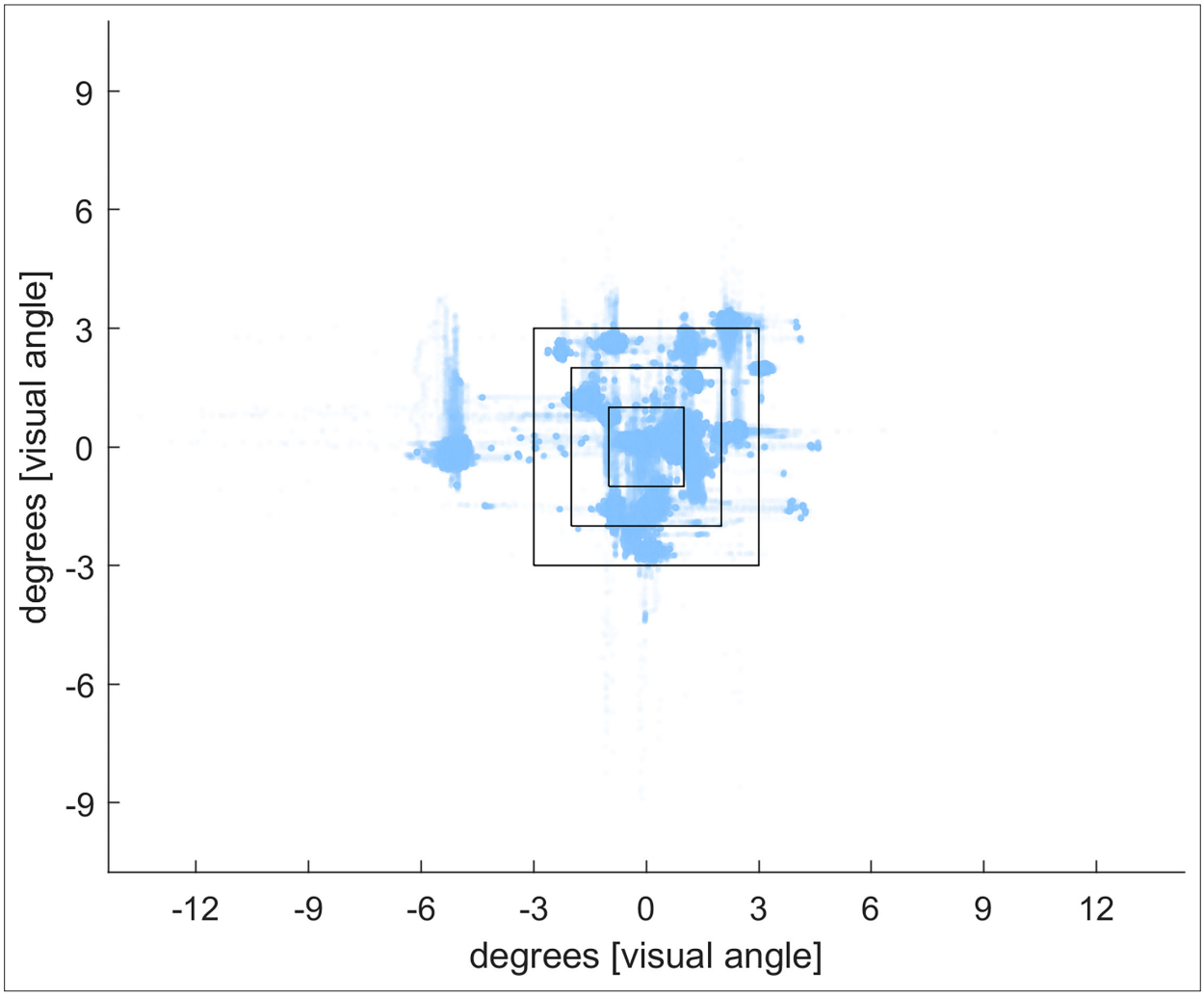

Figure 7—figure supplement 1. Illustration of eye-tracking during the cue-to-target interval (2.5 – 0 s before target onset).

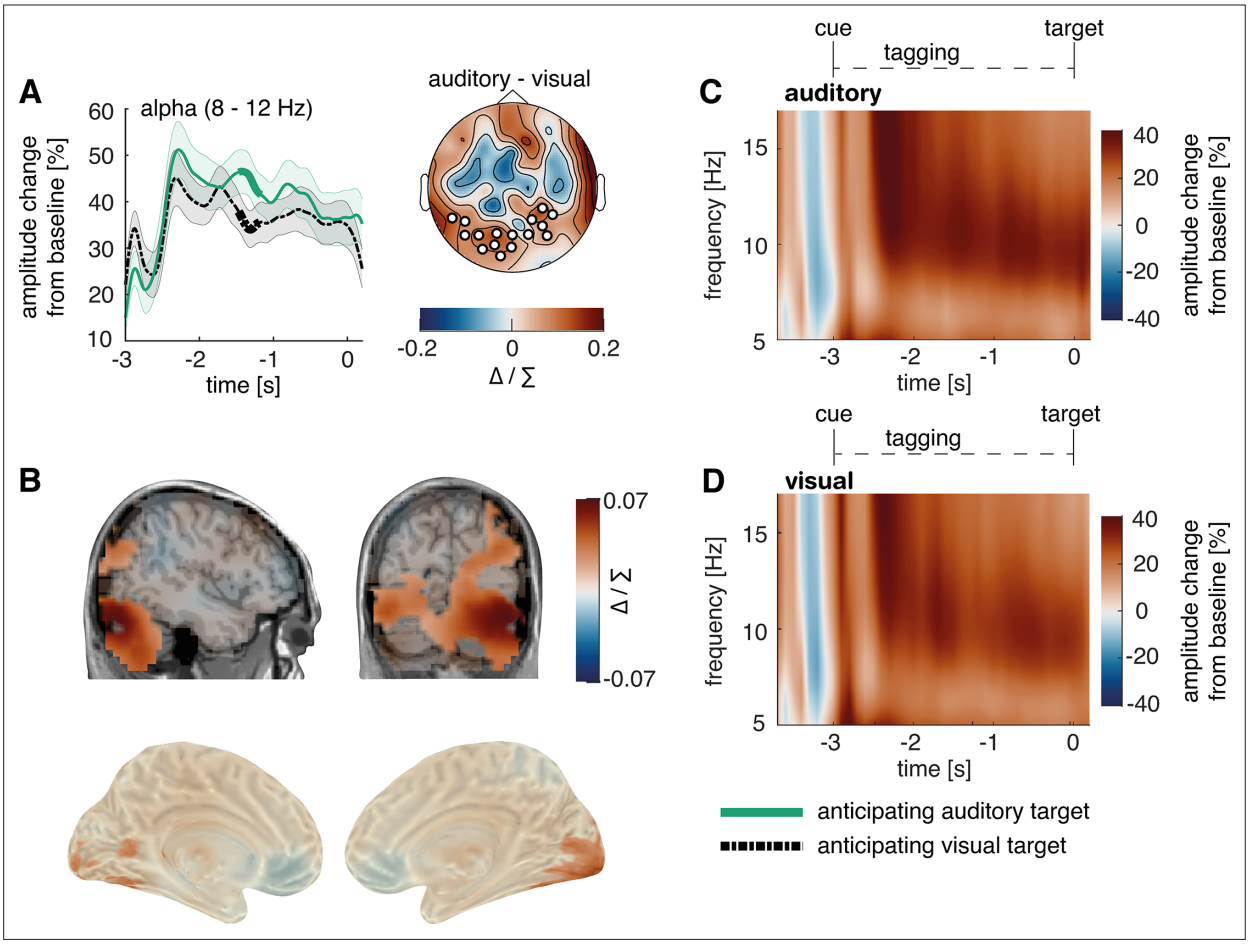

Figure 8. Post-cue modality-specific early visual modulation of alpha power in anticipation of an auditory versus a visual target. (**A**) The time course of post-cue alpha power. Cluster permutation analysis resulted in a condition effect, indicating heightened alpha activity when expecting an auditory compared to a visual target (p=0.034). We found the spectral power of alpha activity, however, not of 36 or 40 Hz to be different between conditions in this electrode cluster (see ***Figure 8—figure supplement 1***). (**B**) Source localisation of the condition difference between expecting an auditory versus a visual target, revealing a significant cluster in early visual areas with stronger effects on the right hemisphere (p<0.01). (**C, D**) Time-frequency representation of power in the cue-to-target interval (average over electrodes that showed maximal condition difference in **A**). *Note:* Cluster electrodes are marked in white. Shading represents standard error from the mean; Δ / ∑ represents (a-b)/(a+b) normalisation.

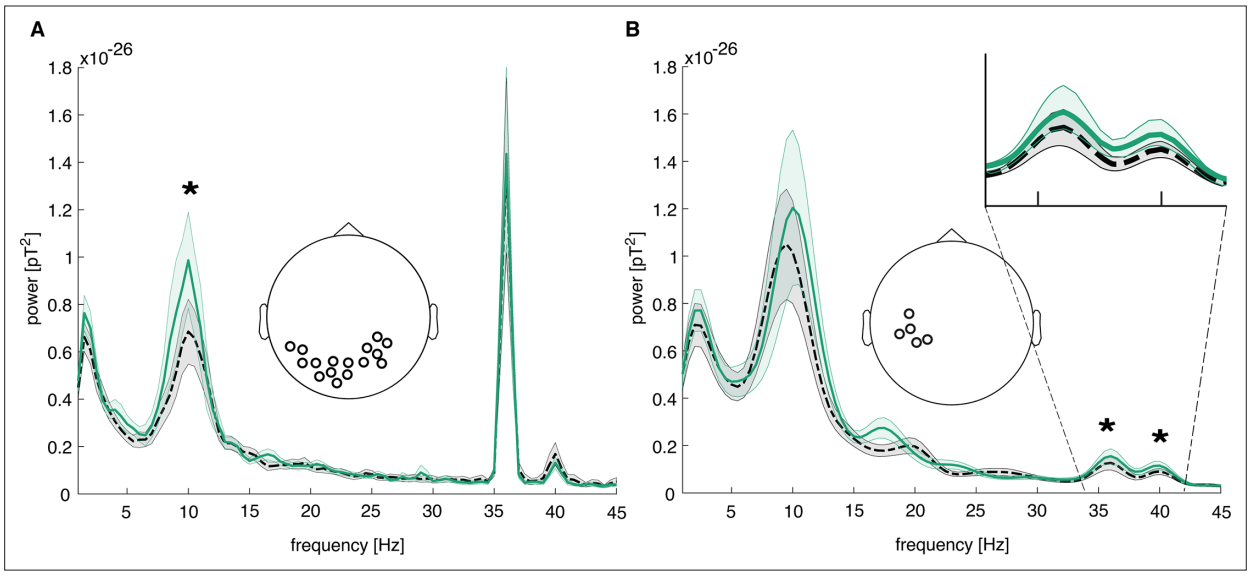

Figure 8—figure supplement 1. Power spectrum over MEG sensor clusters with significant condition differences.

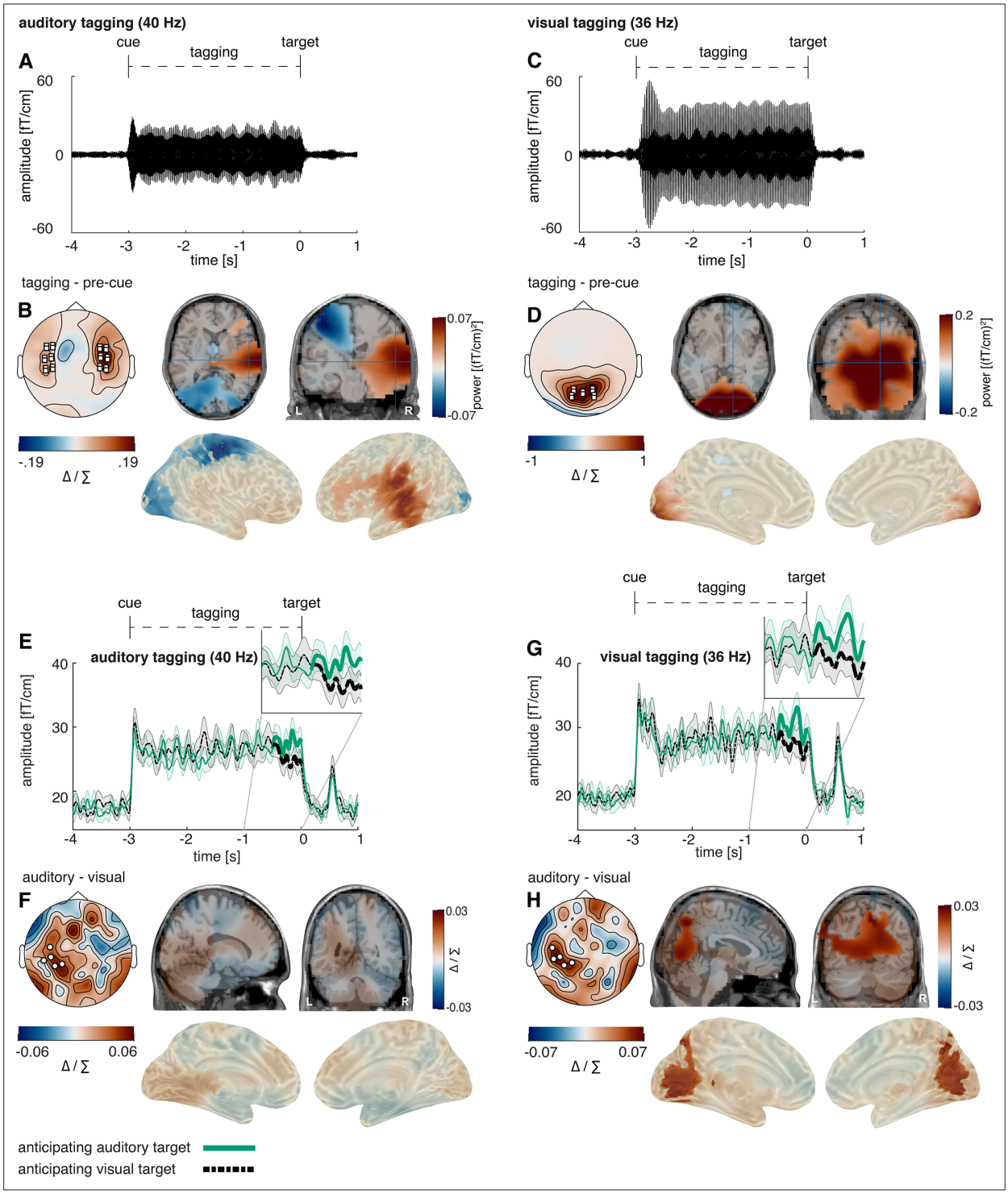

Figure 9. Post-cue modality-specific early visual modulation of alpha power in anticipation of an auditory versus a visual target. (**A**) Auditory steady-state evoked fields (ASSEF) averaged over 24 temporal sensors displaying the highest auditory 40 Hz power (12 right, 12 left; marked in white squares). (**B**) ASSEF source localisation revealed a significant positive cluster in the right-hemispheric early auditory cortex ($p<0.001$). (**C**) Visual steady-state evoked fields (VSSEF) averaged over 10 occipital sensors, displaying the highest visual 36 Hz power (marked in white squares). (**D**) VSSEF source localisation revealed a significant positive cluster in the early visual cortex ($p<0.001$). (**E**) The Hilbert envelope of the 40 Hz ASSEF reveals an increase shortly before target onset when anticipating an auditory compared to a visual target ($p=0.043$); we found the spectral power of 36 Hz and 40 Hz power, but not of alpha power, to be different between conditions in this cluster (***Figure 8—figure supplement 1***). To confirm that 4 Hz difference between the tagged frequencies was sufficient to prevent bleeding over of effects between conditions, we also analysed the Hilbert envelope for 44 Hz when expecting

Figure 9 continued on next page

Figure 9 continued

an auditory target and found no significant condition difference (see ***Figure 9—figure supplement 1***). (**F**) Condition differences in the 40 Hz ASSEF response did not reach significance in sensor space. (**G**) The Hilbert envelope of the 36 Hz VSSEF likewise reveals an increase shortly before target onset when anticipating an auditory compared to a visual target (p=0.019). (**E–G**) For individual power spectra across conditions, see ***Figure 9—figure supplements 2 and 3***. In an additional virtual channel analysis, we found no significant difference between expecting a visual and an auditory target for 36 Hz activity in V1 and for 40 Hz activity in Heschl's Gyrus (see ***Figure 9—figure supplement 4***). (**H**) Condition differences in the 36 Hz VSSEF response were significant over several areas of the visual stream, including most strongly the medial occipital cortex, the calcarine fissure and the precuneus (p=0.047); *Note*: Cluster electrodes are marked in white. Shading represents standard error from the mean. Δ / ∑ represents (a-b)/(a+b) normalisation.

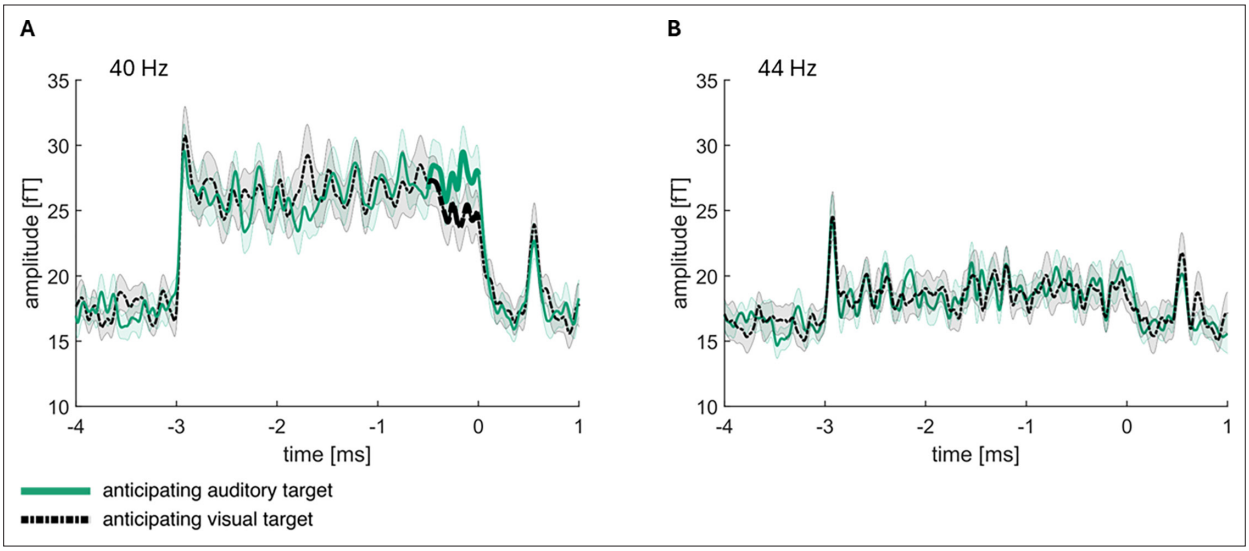

Figure 9—figure supplement 1. Illustration of bleeding over effects over a span of 4 Hz.

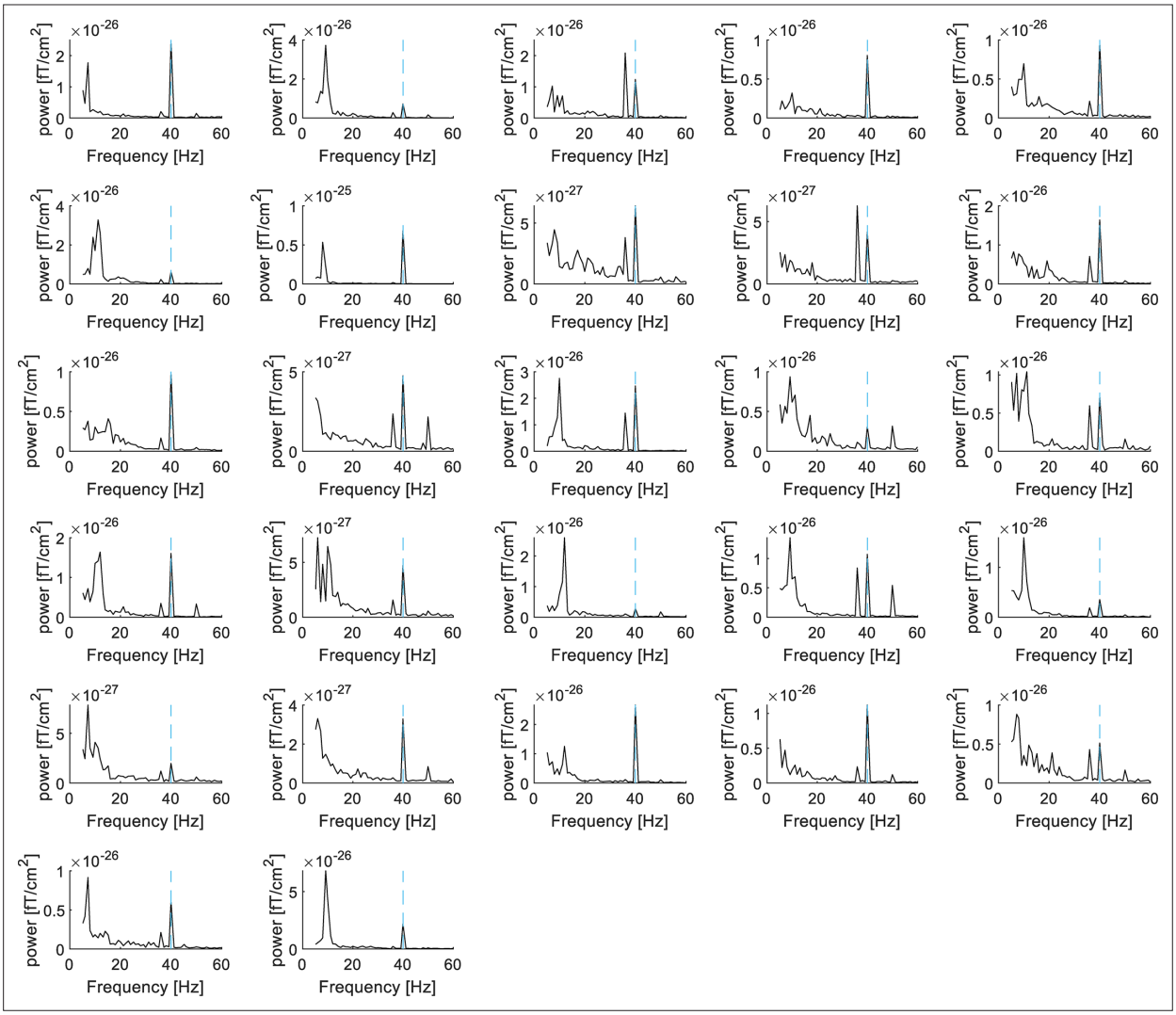

Figure 9—figure supplement 2. Individual ERP power spectra of the cue-to-target interval when anticipating an auditory target in the MEG-study.

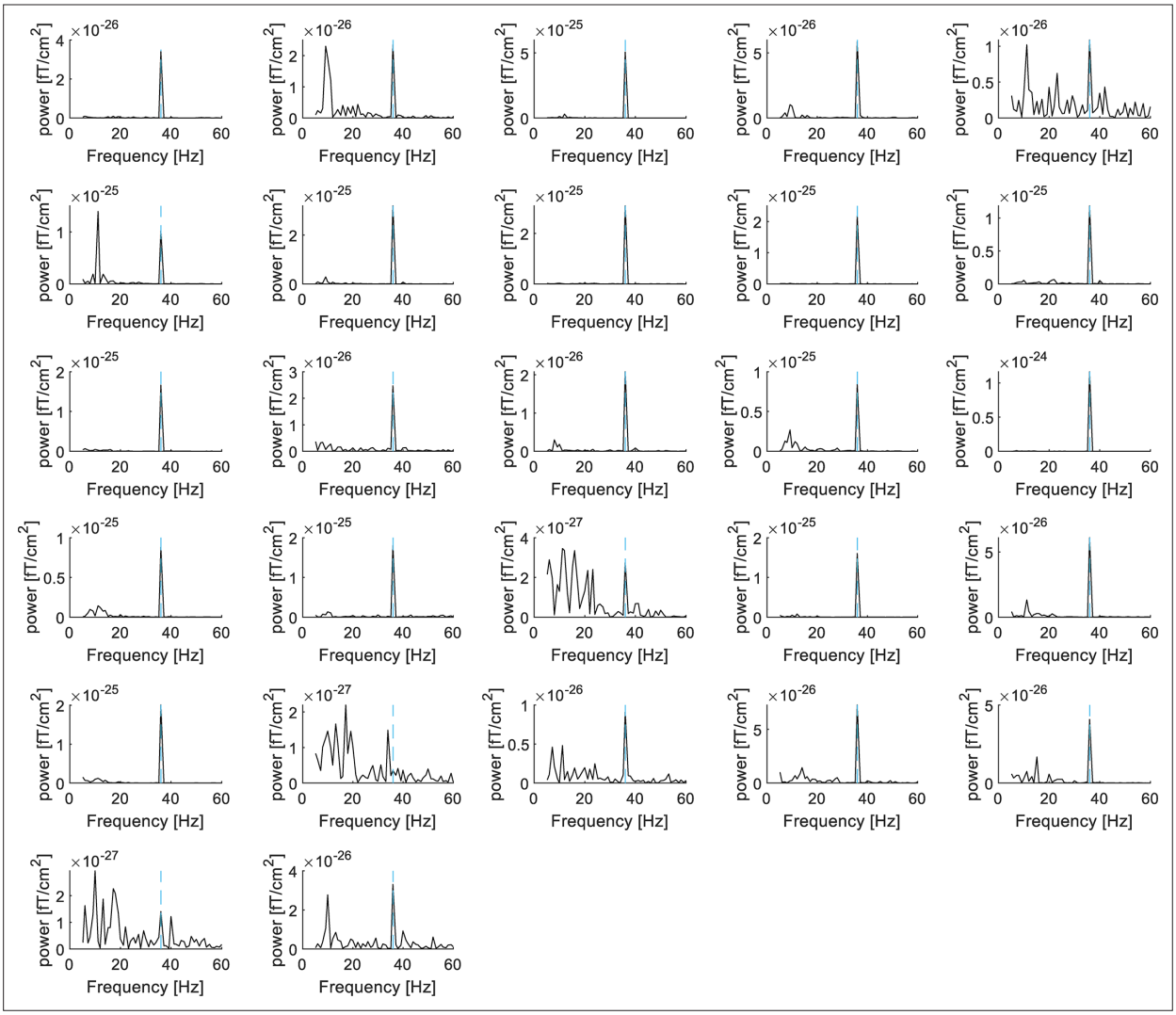

Figure 9—figure supplement 3. Individual ERP power spectra of the cue-to-target interval when anticipating a visual target in the MEG-study.

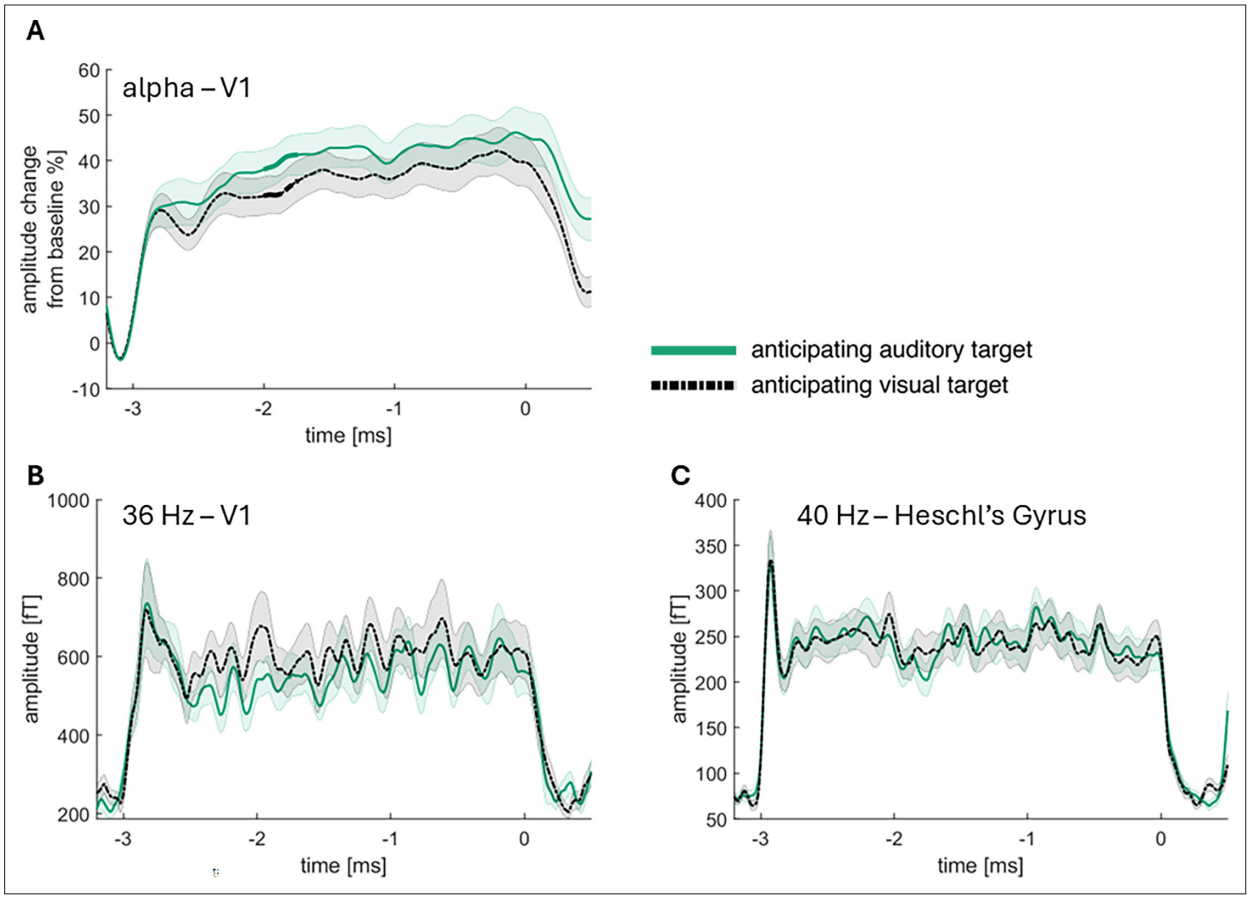

Figure 9—figure supplement 4. Virtual channels for V1 and Helschl's gyrus.

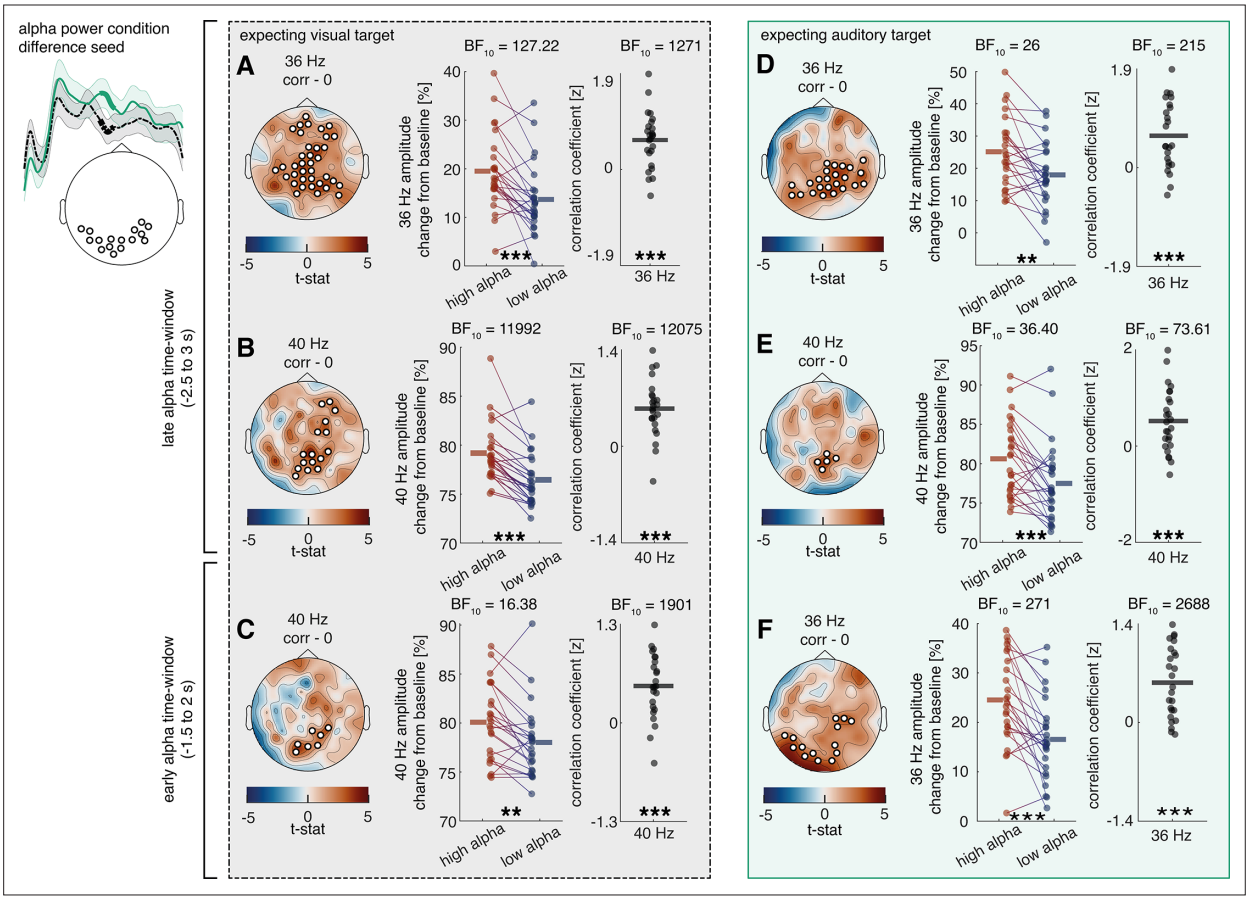

Figure 10. Relationship between cue-induced alpha modulation and amplitude of frequency-tagged responses in study 2. (**A–C**) A positive correlation is visible between alpha activity in the last 500 ms as well as alpha activity in the last 1500–1000 ms and steady state potentials shortly before target onset when expecting a visual target (36 HZ late: p=0.013; 40 Hz late: p=0.009; 40 Hz early: p=002 *popp*). For an exemplary illustration of individual correlations between alpha activity and 36 Hz activity shown in (**A**), see ***Figure 10—figure supplement 1***. (**D–F**) when expecting an auditory target, there is a positive correlation between alpha activity in the last 500 ms as well as alpha activity in the last 1500–1000 ms and steady state potentials shortly before target onset (36 HZ late: p<0.001; 40 Hz late: p=0.005; 36 Hz early: p=011 *popp*). Furthermore, we found a significant correlation between alpha activity as well as 36 Hz SSVEFs with reaction time (see ***Figure 10—figure supplements 2 and 3***). Additionally, we showed that for the last second before target onset, we found significant correlations between the alpha cluster (localised to early visual areas) and 36 Hz activity (over a separate cluster) when expecting an auditory target. When correlating alpha activity with 36 Hz activity within the same early visual electrode cluster, no clear effect was found (see ***Figure 10—figure supplement 4***) N=27; *** sig <0.001; ** sig.<0.01; * sig.<0.05.+sig.<0.1.

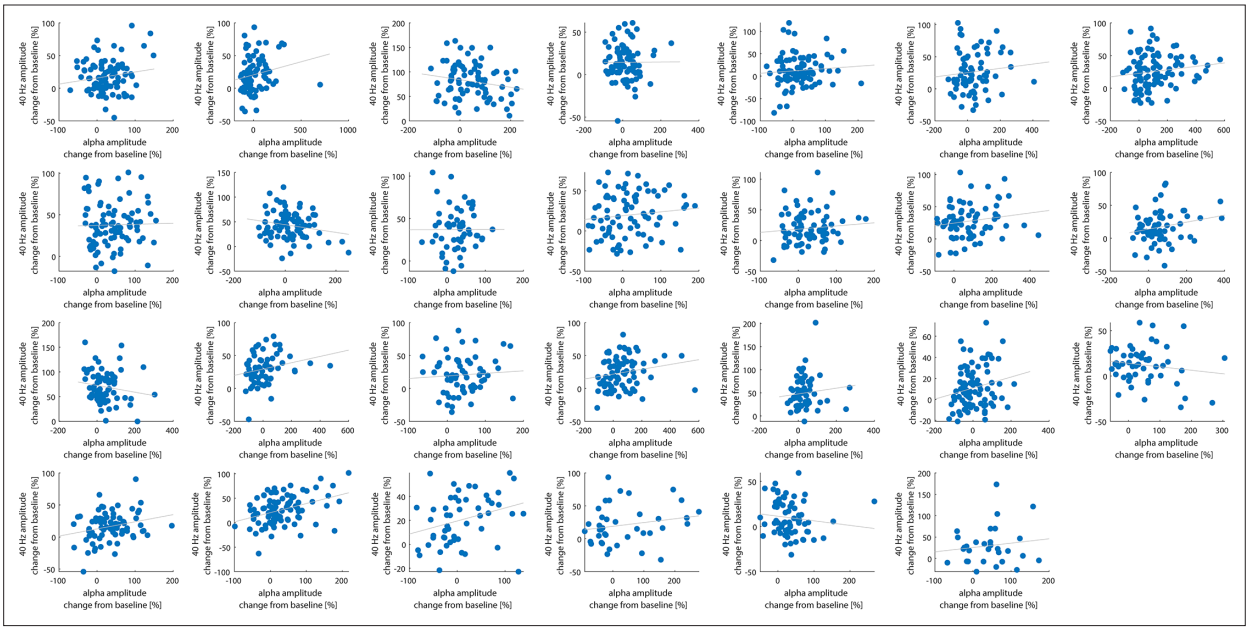

Figure 10—figure supplement 1. Exemplary illustration of the correlation between alpha power (0.5 – 0 s before target onset) and 36 Hz steady-state response (0.5 – 0 s before target onset) for each participant in block 2 (distractors present) when expecting a visual target.

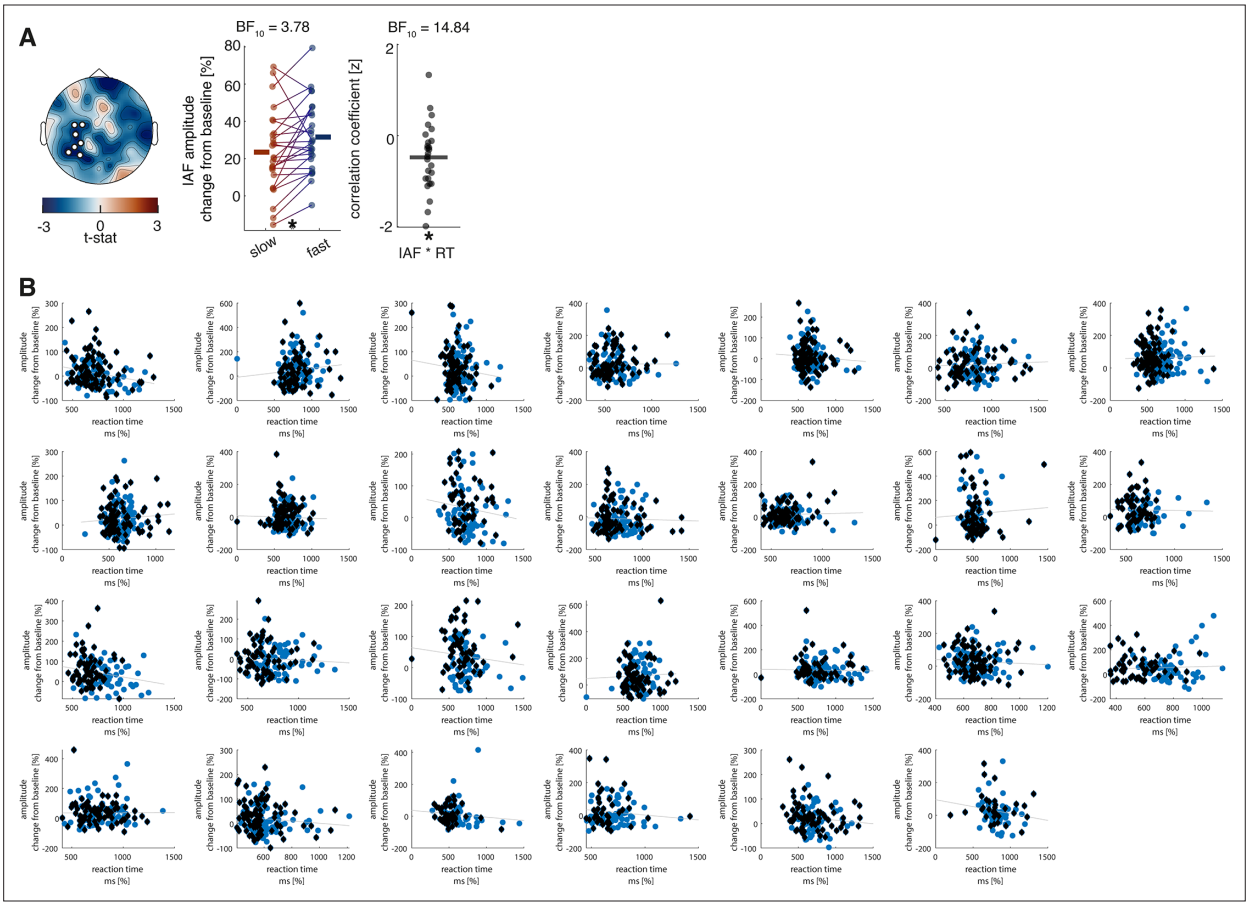

Figure 10—figure supplement 2. Correlation of prestimulus alpha change from baseline with reaction time in the MEG study.

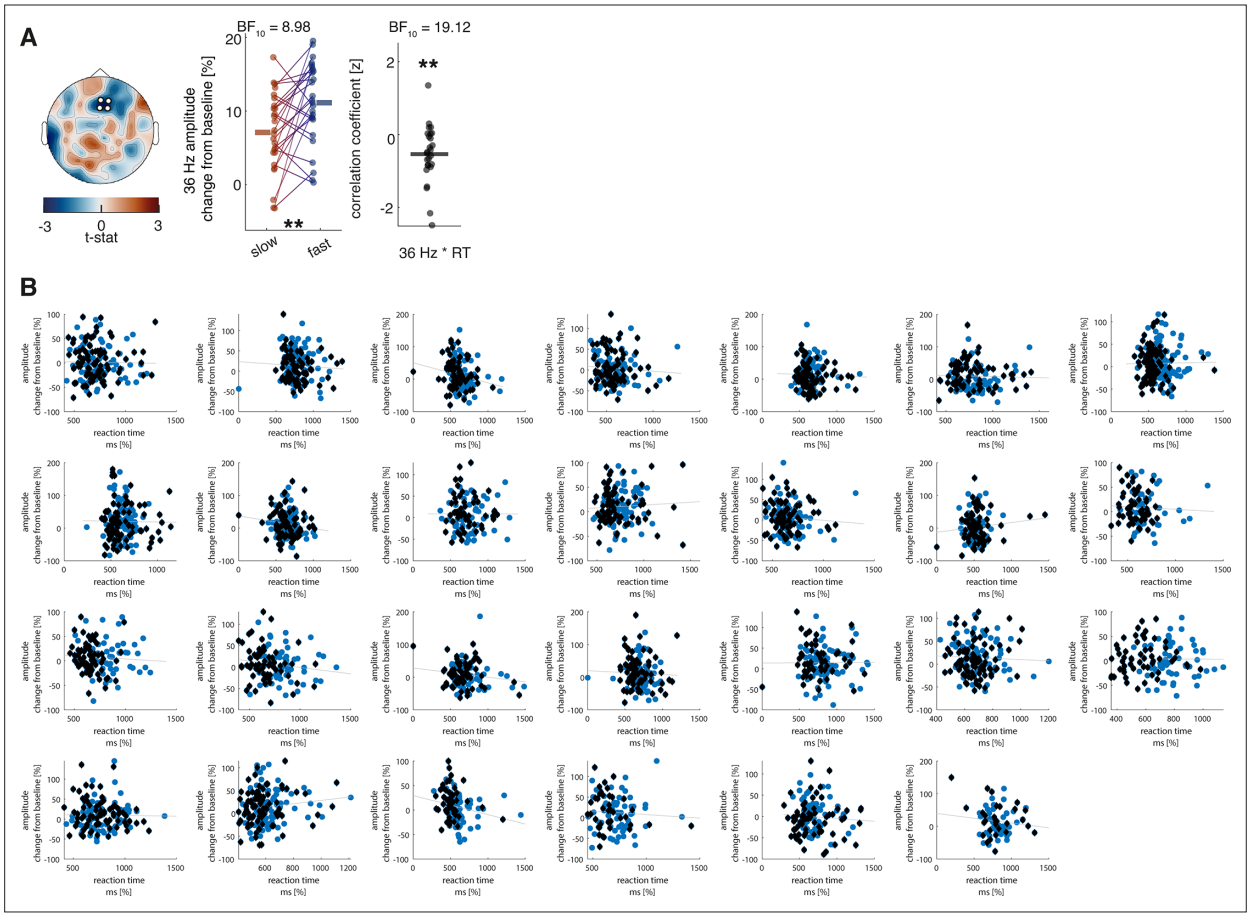

Figure 10—figure supplement 3. Correlation of 36 Hz change from baseline with reaction time in the MEG study.

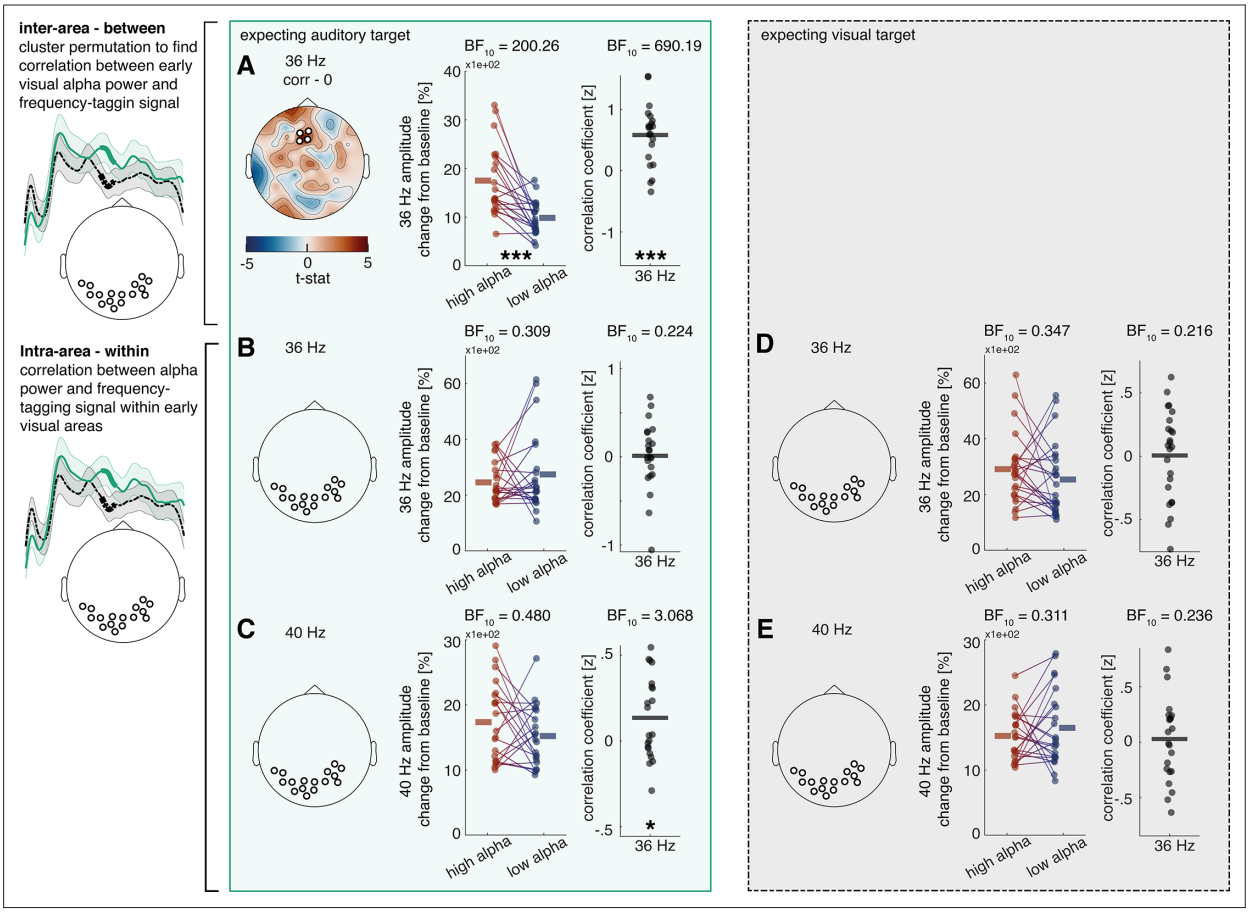

Figure 10—figure supplement 4. Relationship between cue induced alpha modulation and amplitude of frequency tagged responses in the MEG study, both inter- and intra-cortically.

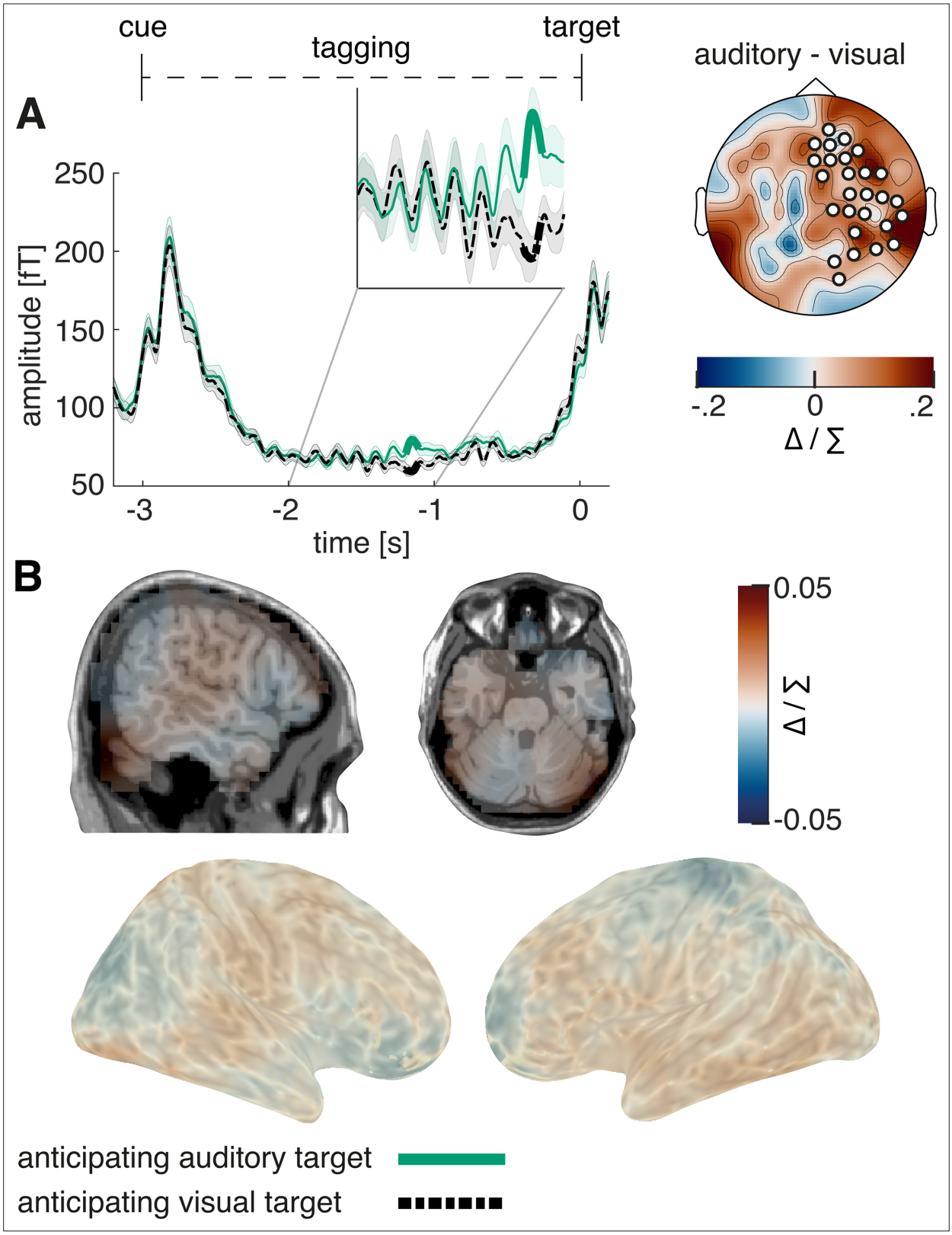

Figure 11. Steady-state response in the intermodulation frequency. (**A**) Similar to study 1, 4 Hz frequency-tagging activity was increased shortly before target onset when expecting an auditory compared to a visual target (p=0.006). (**B**) Source localisation showed activity over auditory sensory areas, but did not reach significance. N=27.